ROBOT LOCALIZATION AND PATH PLANNING BASED ON POTENTIAL FIELD FOR MAP BUILDING IN STATIC ENVIRONMENTS

Y. Yi* **– Z. Wang**

Faculty of Automation and Information Engineering, Xi'an University of Technology, Xi'an 710048, China

ARTICLE INFO

***Article history*:**
Received: 20.07.2014.
Received in revised form: 18.12.2014.
Accepted: 24.12.2014.

Keywords:
Potential Field
Simultaneous Localization and Mapping
Path Planning
Robot

Abstract:

In static environments, and regarding the landmarks also as obstacles in the given situation, this paper suggests a map building algorithm of simultaneous localization and path planning based on the potential field. The robot can locate its movement control discipline with the help of a potential field theory and by conducting simultaneous localization and mapping; besides, the following prediction and state estimation will be done based on predicted control law. With the method of path planning in the potential field, the minimum influential range of space obstacles with repulsive potential can be adjusted, which is in adaptation to the landmarks and environments in which the landmarks are simultaneously regarded as obstacles. The experiments show that the suggested algorithm, through which the robot can conduct simultaneous localization and mapping in the localized landmarks, is also at the same time used as an obstacle in environments. After analyzing relevant performance indicators, the suggested algorithm has been verified as consistent estimation.

1 Introduction

The robot simultaneous localization and mapping (SLAM) is the prerequisite and basis for navigation. The robot navigation means it can independently choose the best path to reach the target location without collision with the obstacles. The robot navigation needs to handle three issues: environmental modeling and robot localization, handling the obtained information and locating the optimal path with collision avoidance. The related issues to the robot SLAM have been extensively studied [1-9], which include state-space presentation of the system, computational complexity, data association, environmental presentation and consistency estimation, and so on. Bailey [4] has discussed and analyzed the consistency estimation affecting EKF-SLAM algorithm. Also, Bailey [5] has analyzed the consistency estimation of Fast-SLAM algorithm. Bosse and Pinies [6, 8] have studied large-scale SLAM. In [7], the compressed EKF estimator produces an estimate that is identical to the EKF estimate but its computational cost can be remarkably lower. So, the CEKFSLAM algorithm

* Corresponding author.
E-mail address: yingminyi@126.com

has solved the problem of constantly expanding state. In [10], the large global covariance is avoided by performing high-frequency operations in a local coordinate frame so as to be more numerically stable and less affected by linearization errors. In [11], the measurement uncertainty is solved. However, all of these studies haven't considered the robot path planning issue.

The SLAM issue considers path planning belongs to the detection planning SLAM issue [12-15, 19]. In [12], the robot motion planning and SLAM issues are constituted into one joint function. Based on this function, the robot plans an optimal path between its current location and a selected local destination in order to implement the whole navigation process in an active and intelligent way. In [15], a novel motion planning approach is proposed for SLAM in out-door. This approach uses the frontier based exploration strategy to find frontier points, and to select the best one as the destination point of the robot. In [9], the robot performs navigation according to the map described as a combination of the topological corridor and metric room maps. This method has combined path planning and the SLAM issue, yet it is only applicable in the surroundings like office. In [11], measurements from a stereo vision camera system and a 2D laser range finder are fused to dynamically plan and navigate a mobile robot. This is a method for avoiding obstacles only but not an optimal path planning method.

To deal with SLAM issue in the obstacle environments, this paper suggests a SLAM algorithm with path planning based on the potential field. When robot simultaneously conducts localization and mapping, the motion control law is determined on the principle of potential field. According to the derivative control law, the next step prediction and state estimation is performed. In path planning methods based on the potential field, the minimum distance of influence of the repulsive potentials identified as obstacles can be adjusted so as to be adaptable to environments with objects characterized by both landmarks and obstacle. This realizes the robot navigation independently in obstacle environments and simultaneous localization and mapping, which improves adaptability and autonomy of robots.

2 System description

The described SLAM system state is formed by the robot's pose and the observed coordinates of the landmarks in the static environments. The joint state vector at the k th moment is shown as:

$$\mathrm{x}_k = \left[x_{vk}, y_{vk}, \theta_{rk}, x_1, y_1, \cdots, x_N, y_N\right]^{\mathrm{T}} = \begin{bmatrix} \mathrm{x}_{vk} \\ \mathrm{n} \end{bmatrix} \quad (1)$$

In (1), $x_{vk}, y_{vk}, \varphi_{vk}$ stand for the position and heading of the robot in two-dimensional space, respectively. The map is static. Notice that the map parameters $\mathrm{n} = \left[x_1, y_1, \cdots, x_N, y_N\right]^{\mathrm{T}}$ do not have a time subscript as they are modeled as stationary. The robot's movement model is rolling motion constraints (i.e., assuming zero wheel slip) [16].

$$\mathrm{x}_k = f_v(\mathrm{x}_{vk-1}, \mathrm{u}_k) = \begin{bmatrix} x_{vk-1} + v_k \Delta T \cos(\theta_{rk-1} + G_k) \\ y_{vk-1} + v_k \Delta T \sin(\theta_{rk-1} + G_k) \\ \theta_{rk-1} + \frac{v_k \Delta T}{B} \sin(G_k) \end{bmatrix} \quad (2)$$

In (2), the time interval between $k-1$ and k is ΔT, the velocity v_k and steering angle G_k are constants and they consist of the controlled vector $\mathrm{u}_k = \left[v_k, G_k\right]^{\mathrm{T}}$. The wheelbase between the front and rear axles is B.

The observation model is given by [16]

$$\mathrm{z}_{ik} = h_i(\mathrm{x}_k) = \begin{bmatrix} \sqrt{(x_i - x_{vk})^2 + (y_i - y_{vk})^2} \\ \arctan\frac{y_i - y_{vk}}{x_i - x_{vk}} - \theta_{rk} \end{bmatrix} \quad (3)$$

3 Slam algorithm with path planning based on potential field

The algorithm combines path planning and simultaneous localization and mapping. The robot SLAM is a process of recursive iteration including prediction, observation, data association, update, and state augmentation. The law of robot motion control is determined by path planning based on the principle of potential fields. According to derivative control law, next step prediction and state estimation is performed. Iterative recursive

estimation is conducted based on the above process. The algorithm diagram is shown in Figure1.

3.1 Path Planning based on Potential Field

When considering environmental landmarks as obstacle and when it has a certain size, the potential function derived from the observed distance can be applied into robot path planning because the potential field is the distance function between objects. The basic idea of path planning based on potential field is as follows. The robot is attracted by waypoint and the observed landmarks as obstacles are excluded at the same time. Robot path planning is shown in Figure 2. In Figure 2, based on a single landmark, the suggested method can develop many landmarks in environments. The robot's movement direction is driven by the waypoint. The robot's speed is direction v_r, the steering angle is θ_r, the relative position from robot to landmarks is p_{rl}, the angle is θ_{rl}, the relative position from robot to waypoint is p_{rw}, its angle is θ_{rw}.

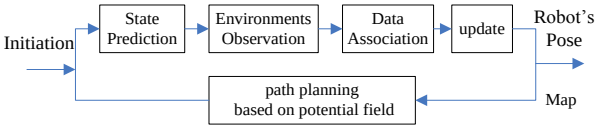

Figure 1: Algorithm Diagram.

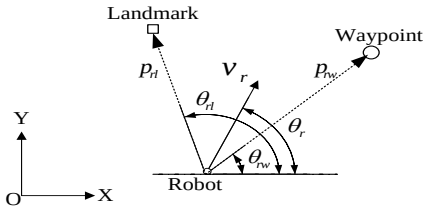

Figure 2: Path Planning.

Here, $p_{rw}=[x_{rw} \quad y_{rw}]^{\mathrm{T}}$, $p_{rl}=[x_{rl} \quad y_{rl}]^{\mathrm{T}}$. The Euclidean distance from robot to landmark is $\|p_{rl}\|$, the Euclidean distance from robot to waypoint is $\|p_{rw}\|$. The defined attractive potential is U_{att} and the repulsive potential is U_{rep} [15].

$$U_{att}=\tfrac{1}{2}\xi_1\|p_{rw}\|^2 \tag{4}$$

$$U_{rep}=\begin{cases}\tfrac{1}{2}\xi_2(\|p_{rl}\|^{-1}-\rho_0^{-1})^2 & \text{if } \|p_{rl}\|\le\rho_0\\ 0 & \text{else}\end{cases} \tag{5}$$

$$U=U_{att}+U_{rep} \tag{6}$$

In the above formula, ρ_0 stands for the tolerant minimum distance between the robot and obstacle landmarks, ξ_1 is the scaling factors for attractive potentials, and $\xi_1>0$, ξ_2 is the scaling factors for repulsive potentials and $\xi_2>0$. If more landmarks as obstacles in the environments, the joint potentials is

$$U=\tfrac{1}{2}\xi_1\|p_{rw}\|^2+\sum_{i=1}^{n}\tfrac{1}{2}\xi_2(\|p_{rl_i}\|^{-1}-\rho_0^{-1})^2 . \tag{7}$$

When the Euclidean distance from robot to obstacle is $\|p_{rl}\|<\rho_0$, robot path planning should make $\dot{p}_{rw}$ pointing to U negative gradient direction by the steepest descent control [16], when

$$\begin{aligned}&\frac{1}{\|\dot{p}_{rw}\|^3}\left(\frac{\partial U}{\partial x_{rw}}\dot{y}_{rw}-\frac{\partial U}{\partial y_{rw}}\dot{x}_{rw}\right)\times\\ &\left(\dot{y}_{rw}\frac{\partial\dot{x}_{rw}}{\partial\theta_r}-\dot{x}_{rw}\frac{\partial\dot{y}_{rw}}{\partial\theta_r}\right)=0\end{aligned}, \tag{8}$$

$\frac{\partial U}{\partial p_{rw}}\frac{p_{rw}}{\|\dot{p}_{rw}\|}$ reaches its minimum.

Formula (9) can be drawn from the joint formula (7) and (8).

$$\begin{aligned}&\|v_r\|\sin\theta_r\left(\xi_1 x_{rw}-\sum_{i=1}^{n}\eta_i x_{rl_i}\right)=\\ &\|v_r\|\cos\theta_r\left(\xi_1 y_{rw}-\sum_{i=1}^{n}\eta_i y_{rl_i}\right)\end{aligned} \tag{9}$$

In the above formula, $x_{rw}=\|p_{rw}\|\cos\theta_{rw}$, $y_{rw}=\|p_{rw}\|\sin\theta_{rw}$, $x_{rl_i}=\|p_{rl_i}\|\cos\theta_{rl_i}$, $y_{rl_i}=\|p_{rl_i}\|\sin\theta_{rl_i}$.

We have

$$\theta_r=\arctan\frac{\sin\theta_{rw}-\sum_{i=1}^{n}\beta_i\sin\theta_{rl_i}}{\cos\theta_{rw}-\sum_{i=1}^{n}\beta_i\cos\theta_{rl_i}} \tag{10}$$

Here,
$\theta_{rw} \neq \theta_{rl_i}$, $\beta_i = \frac{\eta_i \|p_{rl_i}\|}{\xi_1 \|p_{rw}\|}$, $\|p_{rw}\| \neq 0$, $\eta_i = \xi_2 \|p_{rl_i}\|^{-3} (\|p_{rl_i}\|^{-1} - \rho_0^{-1})$.
When $\|v_r\| = \xi_1 \|p_{rw}\|$, also $\dot{U} < 0$ and $U \geq 0$. Thus, when $\|p_{rl_i}\| \leq \rho_0$, in path planning based on potential field, the speed is

$$\|v_r\| = \xi_1 \|p_{rw}\| . \quad (11)$$

The steering angle is shown in the formula (10).

3.2 SLAM Algorithm with Path Planning based on Potential Field

Six steps in each recursive process will be performed for robot SLAM. These procedures are followed by determining the robot's control law, state prediction, environments observation, data association, update and map building.

Step 1: Determine the robot's control law
Path planning means mainly planning the robot's speed and steering angle. The method of planning the robot's speed and steering angle follows Section 3.1 above. As there is no relative to ρ_0 in planning speed formula (11), this paper considers only planning the steering angle. The parameters ρ_0 and ξ_2 in planning the steering angle formula (10) are applicable to adjusting the robot's path planning. As a result, this path planning is classified into two situations:
If all the observed landmarks follow $\|\boldsymbol{p}_{rl_i}\| > \rho_0$, then robot steering angle planning is $\theta_r = \theta_{rw}$,and also follow

$$\theta_{rw} - \theta_{rk-1} - G_{k-1} < G_{\max} . \quad (12)$$

If all the observed landmarks follow $\|p_{rl_i}\| \leq \rho_0$, then robot steering angle planning is θ_r, and also it follows:

$$\theta_r - \theta_{rk-1} - G_{k-1} < G_{\max} . \quad (13)$$

Here, θ_r is calculated from the formula (10). When calculating the formula (10), $\|p_{rl_i}\|$ and $\|p_{rw}\|$ are calculated from the updated landmarks and the robot's position at $k-1$ moment.

Step 2: State prediction
State prediction is fulfilled through the process model in the formula (2).

$$\begin{aligned} \hat{\mathrm{x}}_{k|k-1} &= \mathrm{F}_{k-1}\mathrm{x}_{k-1} \\ \mathrm{P}_{k|k-1} &= \mathrm{F}_{k-1}\mathrm{P}_{k-1|k-1}(\mathrm{F}_{k-1})^T + \mathrm{Q}_{k-1} . \end{aligned} \quad (14)$$

Step 3: Environments observation
Environments observation needs to accomplish the detection of environments characteristics information. The robot position information is calculated through the observation model in the formula (3).

Step 4: Data Association
In the algorithm, the acquired map is a two-dimensional planar map. The Nearest Neighbor method is adopted in data association by Singer et al [17]. The observation z is decomposed into association z_k and observation z_{nk} of new landmarks.

$$\mathrm{z} = \begin{bmatrix} \mathrm{z}_k \\ \mathrm{z}_{nk} \end{bmatrix} . \quad (15)$$

Step 5: Update
State vector and covariance matrix are updated as follows:

$$\begin{aligned} \hat{\mathrm{x}}_{k|k} &= \hat{\mathrm{x}}_{k|k-1} + \mathrm{K}_k(\mathrm{z}_k - h(\hat{\mathrm{x}}_{k|k-1})) \\ \mathrm{P}_{k|k} &= \mathrm{P}_{k|k-1} - \mathrm{K}_k\mathrm{H}_k\mathrm{P}_{k|k-1} \\ \mathrm{K}_k &= \mathrm{P}_{k|k-1}(\mathrm{H}_k)^{\mathrm{T}}(\mathrm{H}_k\mathrm{P}_{k|k-1}(\mathrm{H}_k)^{\mathrm{T}} + \mathrm{R}_k)^{-1} , \end{aligned} \quad (16)$$

Step 6: Map building
The map is built as follows:

$$\begin{aligned} \mathrm{x}_k^{\mathrm{new}} &= h^{-1}(\mathrm{z}_{nk}, \mathrm{x}_{vk}) \\ \mathrm{x}_k &= \begin{bmatrix} \mathrm{x}_k \\ \mathrm{x}_k^{\mathrm{new}} \end{bmatrix} \end{aligned} , \quad (17)$$

For the proposed algorithm, the estimation issue of consistency should be considered. For linear Gaussian filter, the filter performance can be characterized through NEES (normalized estimation error squared) [18].

$$\varepsilon_k = (\mathrm{x}_k - \hat{\mathrm{x}}_{k|k})^{\mathrm{T}} \mathrm{P}_{k|k}^{-1} (\mathrm{x}_k - \hat{\mathrm{x}}_{k|k}) , \quad (18)$$

Under the hypothesis that the filter is consistent and approximately linear-Gaussian, NEES obeys χ^2 distribution. Consistency of the algorithm is evaluated by performing N times Monte Carlo runs. The algorithm performance indicators are evaluated by the average NEES. When $N \to \infty$, $\bar{\varepsilon}_k$ approaches the state vector dimension.

$$\bar{\varepsilon}_k = \frac{1}{N} \sum_{i=1}^{N} \varepsilon_{ik} \quad (19)$$

Given the hypothesis of a consistent linear-Gaussian filter, $N\bar{\varepsilon}_k$ has a χ^2 density with N dim (x_k). Thus, for the 3-dimensional robot pose, with N=50, the 95% probability concentration region for $\bar{\varepsilon}_k$ is bounded by the interval [2.36, 3.72]. If $\bar{\varepsilon}_k$ rises significantly higher than the upper bound, the filter is optimistic and if it tends below the lower bound, the filter is conservative.

4 Experimental results and discussion

The experiment environment is an area, where some landmarks are distributed randomly, and seven waypoints are used to lead the robot's direction, as shown in Figure 3. The two landmarks possess a certain feature of the shape and size and one landmark of radius is $1.3m$, the other landmark of radius is $1.6m$, others are regarded as points without shape and size. In Figure3, "*" denotes landmarks, " Δ " denotes robot, " O " denotes landmarks with shape and size, " • " denotes waypoint, "+" denotes estimated position of the landmarks, "†" denotes landmark's covariance, "-" denotes estimated position of the robot. In Figure3, (a) is the simulation diagram adopting classical EKF-SLAM algorithm, (b) is the simulation diagram adopting classical Fast-SLAM algorithm.

From Figure 3(a), as the robot simultaneous localization and mapping in the environments, the robot's path crosses with two landmarks possessing a shape. This is because the robot still follows the preinstalled waypoint to control its direction angle when it has observed two landmarks with shape and size, which shows that the robot has collided with such landmarks. In Figure 3(b), Fast-SLAM algorithm is adopted, the estimated landmark's covariance is reduced, but the robot's path crosses with two landmarks with shape and size, which shows that the robot has collided with such landmarks. These algorithms haven't considered the case of treating the landmarks as the obstacle at the same time, thus the robot cannot have self-positioning and mapping.

In order to verify the validity of the algorithm, the suggested algorithm is adopted to conduct SLAM simulation, and the consistency estimation of the algorithm is analyzed.

4.1 SLAM simulation with path planning based on potential field

Figure 4 is the SLAM simulation diagram of robot path planning when the potential parameter varies. Simulation is conducted under three conditions: condition one: $\rho_0 = 3$, $\xi_2 = 2$, condition two: $\rho_0 = 3$, $\xi_2 = 12$,condition three: $\rho_0 = 12$, $\xi_2 = 2$.

Figure 5 is the distance curve when the robot is distant from the circular landmarks with radius of $1.3m$ when the parameters vary. The diagram shows the distance curve under three kinds of parameters, respectively.

As Figure 5 shows, three curves are all above $1.3m$, which shows that the distance between the robot and the $1.3m$ -radius circular landmarks is always longer than $1.3m$, and consequently, this means no collision will occur. Under the two conditions when $\rho_0 = 3$, $\xi_2 = 12$ and $\rho_0 = 12$, $\xi_2 = 2$, the curve is obviously higher than the one when $\rho_0 = 3$, $\xi_2 = 2$ after 1000 steps. Figure 5 shows that, the more distant the factor of the potential field ρ_0 is, the sooner the robot gets as far away from obstacle landmarks; the bigger the repulsive factor ξ_2 is, the more obvious the repulsive potential and therefore the more obvious the distance between the robot and the obstacle landmarks. This shows when the robot has observed some landmarks with shape and size and when the robot can adjust potential field distance factor ρ_0 or ξ_2 according to different shape and size; additionally, the robot can avoid colliding with such landmarks by using potential field theory to calculate the robot's control law. Figure 6 is the curve of the robot steering angle when parameters vary. The diagram shows the robot steering angle curve under three kinds of parameters respectively.

In Figure 6, the three curves are basically overlapped before passing 784 steps, and the curves are rather smooth, which shows the robot hasn't observed obstacle landmarks on its path. The change of parameters has no influence on the robot's steering angle. While at 784th step, the three curves all show huge mutation, showing the robot has observed the obstacle landmarks, so the robot will be controlled to divert far from this kind of landmarks according to path planning based on the potential field. Under these two conditions of $\rho_0 = 3$, $\xi_2 = 12$ and $\rho_0 = 12$, $\xi_2 = 2$, the robot's steering angle undergoes two huge mutations after passing 800 steps, showing the robot can adjust the potential field distance factor ρ_0 or repulsive factor ξ_2 and adjust the robot's control law to avoid colliding with such landmarks.

4.2 Consistency estimation of the robot poses

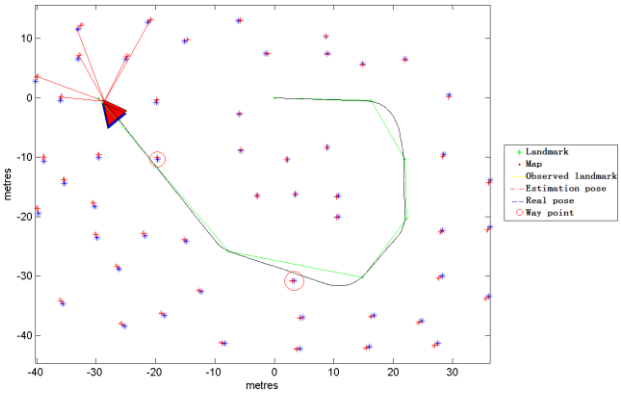

(a) EKF-SLAM algorithm simulation

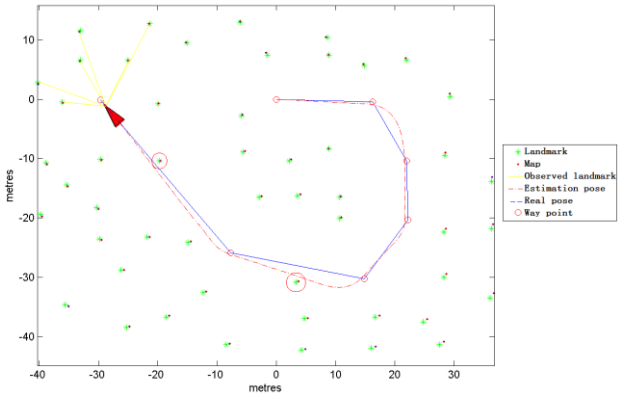

(b) Fast-SLAM algorithm simulation

Figure 3: The robot path with classic SLAM algorithm when encountering shaped obstacles.

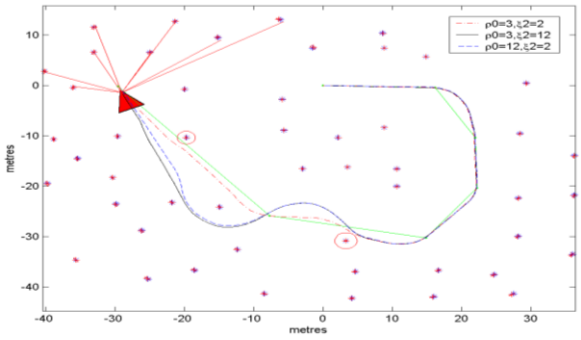

Figure 4: The robot SLAM with path planning based on potential field when parameters vary.

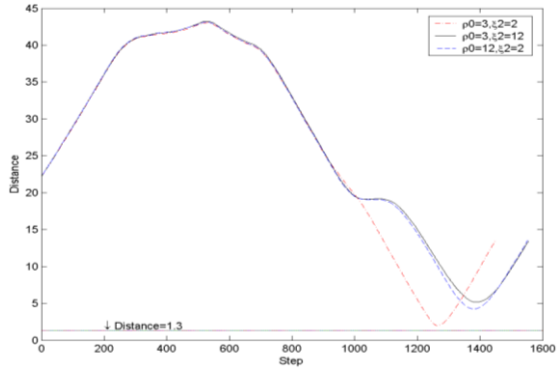

Figure 5: Influence of parameters on distance.

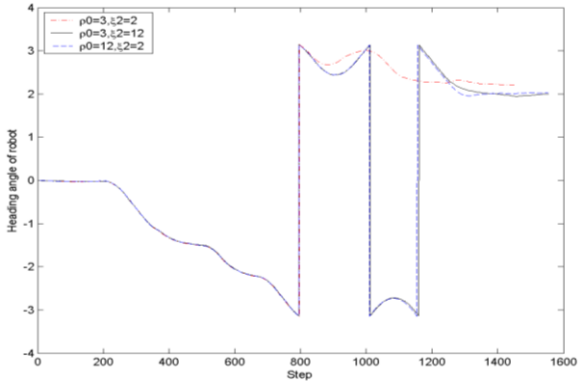

Figure 6: Influence of parameters on the steering angle.

When $\rho_0 = 3$, $\xi_2 = 2$, the suggested algorithm is adopted to run Monte Carlo simulation 50 times,and the average NEES of its pose is shown in Figure 7. From Figure 7, the average NEES of the robot pose all obey χ^2 distribution, and the curve is basically within [2.36, 3.72]. Thus it can treat the algorithm as consistency estimation.

5 Conclusion

To deal with landmark characterized by both landmark and obstacle in unknown environments, a Simultaneous Localization and Mapping algorithm based on path planning is presented. When the robot motion control law is planned for the next step based on the potential field theory, the robot can perform simultaneous localization and mapping, adjust the relevant measurement factors according to the observed landmarks with shape and size, determine the robot's control law and avoid obstacles wisely and conduct path planning. The consistency estimation of the suggested algorithm is verified by Average NEES. The algorithm is applicable in static environments, while further studies are needed in dynamic environments.

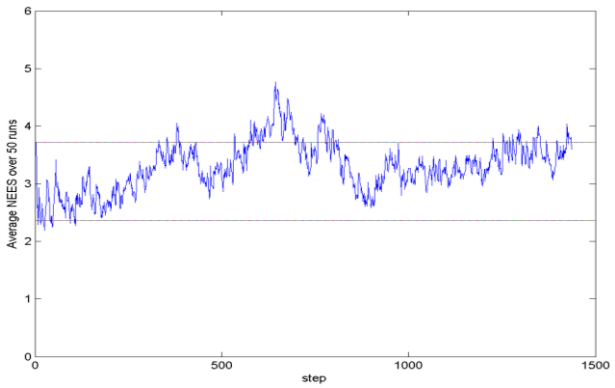

Figure 7: Average NEES of robot's pose.

In dynamic environments, static landmark and dynamic random target exist simultaneously. For such cases, SLAM problem needs to consider the following issues:

(1) In order to build the random target into the map, the trajectory of random targets is to be predicted.

(2)The collisions problem between the robot and random target are considered.

(3) The map is built involving static landmark and dynamic random target.

Acknowledgment

This work was supported by National Natural Science Foundation of China (No. 51275405) and the science research programs of education department of Shaanxi Province (2013JK1078).

References

[1] Davison, A. J., Reid, I. D., Molton, N. D., Stasse, O.: *MonoSLAM: Real-Time Single Camera SLAM*, IEEE Transactions on Pattern Analysis and Machine Intelligence, 29(2007), 6, 1052-1067.

[2] Clemente, L., Davison, A., Reid, I., Neira, J., Tard´os, J. D.: *Mapping Large Loops with a Single Hand-Held Camera*, In Robotics Science and Systems, The MIT Press, Atlanta, Georgia, USA, 2008.

[3] Paz, L. M., Pinies, P., Tardos, J. D., Neira, J.: *Large-Scale 6-DOF SLAM With Stereo-in-Hand*, IEEE Transactions on Robotics, 24(2008), 5, 946-957.

[4] Bailey, T., Nieto, J., Guivant, J., Stevens, M., Nebot, E.: *Consistency of the EKF-SLAM Algorithm*, In IEEE/RSJ International Conference on Intelligent Robots and Systems, Beijing, China, IEEE, 2006, 3562-3568.

[5] Bailey, T., Nieto, J., Nebot, E.: *Consistency of the Fastslam Algorithm*, In Proc. IEEE Intl. Conf. on Robotics and Automation, Orlando, Florida, USA,IEEE, 2006,424-429.

[6] Bosse, M., Newman, P., Leonard, J., Teller, S.: *Simultaneous Localization and Map Building in Large-Scale Cyclic Environments Using the Atlas Framework*, Int. J. Robotics Research, 23(2004), 12, 1113-1140.

[7] Guivant, J., Nebot, E.: *Optimization of the Simultaneous Localization and Map Building Algorithm for Real Time Implementation*, IEEE Transactions on Robotics and Automation, 17(2001), 3, 242-257.

[8] Pinies, P., Tardos, J. D.: *Large-Scale SLAM Building Conditionally Independent Local Maps: Application to Monocular Vision*, IEEE Transactions on Robotics, 24(2008), 5, 1094-1106.

[9] Blanco, J. L., Fernandez-Madrigal, J. A., Gonzalez, J.: *Toward a Unified Bayesian Approach to Hybrid Metric Topological SLAM*, IEEE Transactions on Robotics and Automation, 24(2008), 2, 259-270.

[10] Guivant, J., Nebot, E.: *Improving Computational and Memory Requirements of Simultaneous Localization and Map Building Algorithms*, In IEEE International Conference on Robotics and Automation, Washington, DC, IEEE, 3(2002), 2731-2736.

[11] Thrun, S., Fox, D., Burgard, W.: *A Probabilistic Approach to Concurrent Mapping and Localization for Mobile Robots*, Machine Learning, 31(1998), 29-53.

[12] Chen, D., Zhang, L: *Fuzzy Geometric Maps and Vertex Self-Localization for SLAM Problem*, Control Theory & Application, 23(2006), 5, 679- 686.

[13] Frintrop, S., Jensfelt, P.: *Attentional Landmarks and Active Gaze Control for Visual SLAM*, IEEE Transactions on Robotics, 24(2008), 5,1054-1065.

[14] Smith, R., Self, M., Cheeseman, P.: *Estimating Uncertain Spatial Relationships in Robotics*, In Uncertainty in Artificial Intelligence 2, J.F. Lemmer and L. N. Kanal, Eds. Elsevier, New York, 1988, 435-461.

[15] Ge, S. S., Cui, Y. J.: *New Potential Functions for Mobile Robot Path Planning*, IEEE Transactions on Robotics and Automation, 16(2000),5,615-620.

[16] Vincent, T. L., Grantham, W. J.: *Nonlinear and Optimal Control Systems*, Hoboken John Wiley & Sons, 1997.

[17] Singer, R. A., Sea, R. G.: *A New Filter for Optimal Tracking in Dense Multi-Target Environment*, In Proceedings of the Ninth Allerton Conference Circuit and System Theory, Urbana-Champaign, Univ.of Illinois, USA, 1971,201-211.

[18] Bar-Shalom, Y., Li, X. R., Kirubarajan,T.: *Estimation with Applications to Tracking and Navigation*, John Wiley and Sons, 2001, 234-235.

[19] Krajči, V., Stojković, N.: *Improvement of Robot Trajectory Tracking by Using Nonlinear Control Methods*, Engineering Review, 2006(26),1,7-17.